

DEEP MANIFOLD TRAVERSAL: CHANGING LABELS WITH CONVOLUTIONAL FEATURES

Jacob R. Gardner^{1*}, Matt J. Kusner^{2*}, Yixuan Li¹, Paul Upchurch¹,
Kilian Q. Weinberger¹ & John E. Hopcroft¹

¹Department of Computer Science. Cornell University, Ithaca, NY.

²Department of Computer Science & Engineering. Washington University in St. Louis, St. Louis, MO.
{jrg365, yl2363, pru3, kqw4, jeh17}@cornell.edu
{mkusner}@wustl.edu

ABSTRACT

Machine learning is increasingly used in high impact applications such as prediction of hospital re-admission, cancer screening or bio-medical research applications. As predictions become increasingly accurate, practitioners may be interested in identifying actionable changes to inputs in order to alter their class membership. For example, a doctor might want to know what changes to a patient’s status would predict him/her to not be re-admitted to the hospital soon. Szegedy et al. (2013b) demonstrated that identifying such changes can be very hard in image classification tasks. In fact, tiny, imperceptible changes can result in completely different predictions without any change to the true class label of the input. In this paper we ask the question if we can make small but *meaningful* changes in order to *truly alter the class membership* of images from a source class to a target class. To this end we propose *deep manifold traversal*, a method that learns the manifold of natural images and provides an effective mechanism to move images from one area (dominated by the source class) to another (dominated by the target class). The resulting algorithm is surprisingly effective and versatile. It allows unrestricted movements along the image manifold and only requires few images from source and target to identify meaningful changes. We demonstrate that the exact same procedure can be used to change an individual’s appearance of age, facial expressions or even recolor black and white images.

1 INTRODUCTION

Machine learning is now commonplace in many real-world applications such as autonomous driving (Hadsell et al., 2009), predicting if hospital patients will be readmitted soon (Yu et al., 2013), and automatic carcinoma cancer detection (Cruz-Roa et al., 2013). In many settings, machine learning has progressed as far as being able to surpass human-level predictions (He et al., 2015).

As automatic predictions become increasingly used by practitioners, there will be scenarios where the predicted class label of an input is correct but undesired: a patient has high risk of heart disease, a house is appraised at a low value, a patient is likely to be re-admitted to a hospital. In these settings the practitioner might want to know what actionable changes would transform these outcomes for the better. Typically, these changes should be minimal, to reduce unnecessary or unreasonable cost. For example, the appraisal of a house should change through small modifications of the existing house not by replacing it with a brand new mansion.

This paper focuses on the problem of automatically identifying actionable changes to alter class labels. Little research exists on this topic (Cui et al., 2015). However, recent work (Szegedy et al., 2013b; Nguyen et al., 2014) has demonstrated that this problem can be surprisingly hard in image classification tasks. It is possible to change the *prediction* of an image with tiny alterations that can be *imperceptible to humans* and do not change the *class label* (Szegedy et al., 2013b). In fact, this problem persists for most machine learning algorithms and is not limited to deep neural

*These authors contributed equally.

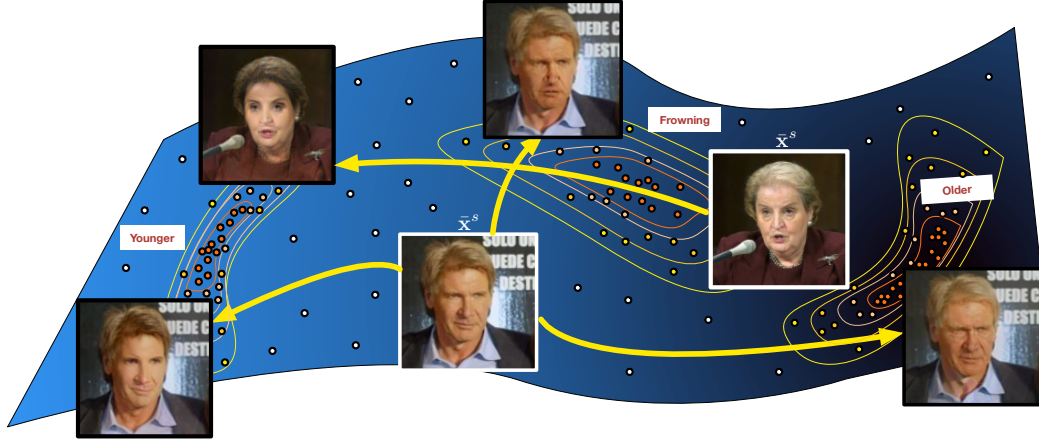


Figure 1: An illustration of several manifold traversals from source images (white border) to various target labels. All target images (black border) are synthetically generated with our method from the respective source images (best viewed in color; zoom in to reveal facial details). The sample target images are represented as colored dots and give rise to the target distribution (orange contours) along the manifold; none of them are from the two subjects. White dots represent ImageNet natural images that were used to learn the global natural images manifold (blue).

networks (Goodfellow et al., 2014). In the scenario of the doctor this means that tiny meaningless changes to the patient’s health record could elevate him/her to be classified as perfectly healthy whereas in reality his/her health status has not changed at all.

In this paper we investigate how to make *meaningful changes* to inputs in order to *truly* change their *class label*. Formally, we are given training inputs from two classes $\mathbf{x}_1^s, \dots, \mathbf{x}_m^s$ all of a *source* class y^s and $\mathbf{x}_1^t, \dots, \mathbf{x}_n^t$ all of a *target* class y^t . Given a test input $\bar{\mathbf{x}}^s$ from class y^s , we would like to find a transformation $\bar{\mathbf{x}}^s \rightarrow \bar{\mathbf{x}}^t$, so that $\bar{\mathbf{x}}^t$ is most similar to the original $\bar{\mathbf{x}}^s$, yet also associates with class y^t . In the spirit of Szegedy et al. (2013b), we pilot our study of actionable change in the context of images, so that our results may be easily visualized to verify the change in class membership.

Manifold Traversal. For high dimensional data to be interesting it must contain low-dimensional structure. Although embedded in very high dimensional pixel spaces, natural images are believed to lie on lower dimensional sub-manifolds (Weinberger & Saul, 2006). One interpretation of the results by Szegedy et al. (2013b) is that if we allow arbitrary movements off the manifold, we can find pockets in space that are associated with any arbitrary label. For example, one could change the *predicted label* of an image of a zebra into a car by drawing imperceptibly faint signature features of cars on top of the zebra. This is challenging for at least two reasons: First, small changes across multiple dimensions tend to add up to large distances overall, making it easy to leave the manifold in high dimensional ambient spaces; Second, we need to move $\bar{\mathbf{x}}^s$ *along the manifold* into a region where the class label y^t is dominant. We address each point.

In this paper we observe that we can extract a good approximation of the low-dimensional data manifold of natural images from deep convolutional representations (Simonyan & Zisserman, 2015) that have been trained on 1.2 million natural images from the ImageNet corpus (Russakovsky et al., 2015). We use the feed forward convolutional network as a mapping onto the manifold, $\phi(\cdot)$, and map our source image onto the new feature representation, $\bar{\mathbf{z}}^s = \phi(\bar{\mathbf{x}}^s)$. Once the manifold is captured, we only require few labeled images from the source and target labels. We map them into the learned feature space and use a distribution membership test based on the Maximum Mean Discrepancy (MMD) (Fortet & Mourier, 1953; Gretton et al., 2012) statistic to find a location $\bar{\mathbf{z}}^t$ close to $\bar{\mathbf{z}}^s$ with high likelihood of class y^t . As our mapping from images to convolutional features is irreversible, we solve a small optimization problem to recover $\bar{\mathbf{x}}^t$ such that $\phi(\bar{\mathbf{x}}^t) \approx \bar{\mathbf{z}}^t$.

The resulting algorithm allows us to traverse the manifold of natural images freely to make actionable changes as long as labeled target images are available. Figure 1 illustrates several manifold traversals of human faces along the manifold of natural images. Although the blue manifold and

the orange distribution contours are drawn for illustration purposes only, all image changes were computed with our algorithm. The figure illustrates the versatility of our approach: As long as there are labeled target images available, our algorithm allows movements along the manifold in any direction. For example, the label of Madeline Albright’s image is changed from “older” to “younger”, and the image of Harrison Ford is changed towards “younger”, “frowning”, and “older”.

2 RELATED WORK

Szegedy et al. (2013b) were the first to show that deep networks can be ‘easily convinced’ that an input is in a different class, by making subtle, imperceptible changes to the input. Such changed inputs were termed ‘adversarial examples’ and Goodfellow et al. (2014) showed that these examples are generally problematic for high-dimensional linear classifiers. These results indicate it is inherently difficult to meaningfully change the label of an input with small changes. Different from this work we make use of a recent non-linear method for label change. Additionally, we modify on high-level convolutional neural network (ConvNet) features to create meaningful changes.

Another work which makes use of the Maximum Mean Discrepancy (MMD) (Gretton et al. (2006)) in a deep network is that of Li et al. (2015). They show that the MMD can be used to construct a generative deep neural model by minimizing the MMD between generated images and real images.

Mahendran & Vedaldi (2015) recovered visual imagery by inverting deep convolutional feature representations. Their goal was to reveal invariances by comparing a reconstructed image to the original image. Gatys et al. (2015) demonstrated how to transfer the artistic style of famous artists to natural images by optimizing for feature targets during reconstruction. We draw upon these works as means to demonstrate our framework in the image domain. Yet, rather than reconstructing imagery or transferring style, we construct new images which have the qualities of a different class.

Changing the class of an image is an important problem. Semantic colorization (Chia et al., 2011) changes a grayscale image into a color image by semantic cues. Images of faces, in particular, have attracted much attention. Methods have been proposed to synthesize new expressions (Kemelmacher-Shlizerman, 2013), make a face older (Kemelmacher-Shlizerman et al., 2014), and change identity (Bitouk et al., 2008). These works inspire our demonstrations on face images. Unlike these methods, our demonstrations do not use any domain-specific information nor do we require any manual annotation.

Perhaps most similar in spirit to our method is recent work on optimal-action extraction in additive tree models Cui et al. (2015). This paper derives an actionable plan to change an input to a certain class via random forests or tree boosting through a linear program. This work can be seen as complimentary to ours.

3 BACKGROUND

Convolutional Networks Convolutional neural networks have achieved dramatic success across a wide range of applications in computer vision, perhaps most prominently in object recognition (Krizhevsky et al., 2012; Sermanet et al., 2013). This success is typically attributed to the ability of ConvNets to learn deep visual feature representations that explicitly capture object-specific information while ignoring noisy information irrelevant to the object category (Donahue et al., 2013; Szegedy et al., 2013a). It has been shown by Donahue et al. (2013) that features extracted from ConvNets have sufficient generalization ability, which tend to cluster images into semantically meaningful categories on which the network was never explicitly trained. Razavian et al. (2014) further extended the results in Donahue et al. (2013), and confirmed the representational power of ConvNets by performing a wide spectrum of visual recognition tasks using the representations from the model of OVERFEAT (Sermanet et al., 2013).

Maximum Mean Discrepancy The *Maximum mean discrepancy* (Fortet & Mourier, 1953) (MMD) statistic tests whether two probability distributions, source P^s and target P^t , are the same. To this end it produces a function that can distinguish samples from these two distributions. In particular, this function is from a class of functions \mathcal{F} that is large when evaluated on samples drawn from a source distribution P^s , and small when evaluated on samples drawn from a target distribution

P^t . The MMD distributions measures the maximum difference between the mean function values:

$$\text{MMD}(P^s, P^t, \mathcal{F}) = \sup_{f \in \mathcal{F}} (\mathbb{E}[f(\mathbf{z}^s)]_{\mathbf{z}^s \sim P^s} - \mathbb{E}[f(\mathbf{z}^t)]_{\mathbf{z}^t \sim P^t}). \quad (1)$$

When \mathcal{F} is a reproducing kernel Hilbert space, the function maximizing this difference can be found analytically, and is called the *witness function*:

$$f^*(\mathbf{z}) = \mathbb{E}[k(\mathbf{z}^s, \mathbf{z}^t)]_{\mathbf{z}^s \sim P^s} - \mathbb{E}[k(\mathbf{z}^s, \mathbf{z}^t)]_{\mathbf{z}^t \sim P^t} \quad (2)$$

The MMD using this function is a powerful measure of discrepancy between two probability distributions. For example, it is easy to show that if \mathcal{F} is universal, then $P^s = P^t$ if and only if $\text{MMD}(P^s, P^t, \mathcal{F}) = 0$ (Gretton et al., 2012).

Given finite samples $\mathbf{z}_1^s, \dots, \mathbf{z}_n^s \stackrel{iid}{\sim} P$ and $\mathbf{z}_1^t, \dots, \mathbf{z}_m^t \stackrel{iid}{\sim} P^t$, the witness function can be estimated empirically:

$$f^*(\mathbf{z}) \approx \sum_{i=1}^n k(\mathbf{z}_i^s, \mathbf{z}) - \sum_{i=1}^m k(\mathbf{z}_i^t, \mathbf{z}) \quad (3)$$

Intuitively, $f^*(\mathbf{z})$ measures the degree to which \mathbf{z} is representative of either P^s — by taking a positive value — or P^t — by taking a negative value. For a more thorough review of the MMD statistic, see Gretton et al. (2012).

4 DEEP MANIFOLD TRAVERSAL

In this section, we will discuss our method for manifold traversal from one class into another. Importantly, any efficient transformation should preserve the class-independent aspects of the original image, only changing the class-identifying features. Our setup is somewhat different than that found in typical supervised learning. In our setting, we are given a labeled set of instances from a *source domain*, $\bar{\mathbf{x}}_1^s, \dots, \bar{\mathbf{x}}_m^s$ each with source label y^s , a set of labeled instances from a *target domain*, $\bar{\mathbf{x}}_1^t, \dots, \bar{\mathbf{x}}_n^t$ each with target label y^t . We are also given a specific *input instance* $\bar{\mathbf{x}}^s$ with label y^s . Informally, our goal is to change $\bar{\mathbf{x}}^s \rightarrow \bar{\mathbf{x}}^t$ in a meaningful way such that $\bar{\mathbf{x}}^t$ has true label y^t . Figure 2 provides an overview of our approach.

Manifold representation. The first step of our approach is to approximate the manifold of natural images and obtain a mapping from input images in pixel space, \mathbf{x} , to a suitable representation on the manifold, $\mathbf{x} \rightarrow \phi(\mathbf{x})$. Traversing this manifold in a meaningful way involves changing objects in these images. This motivates using learned features from a deep convolutional neural network trained to recognize object classes as our manifold learning algorithm. By modifying these deep visual features rather than the raw pixels of \mathbf{x} directly, we make changes to the class of the object of the image.

Network details. Following the method of Gatys et al. (2015) we use the feature representations from deeper layers of a normalized, 19-layer VGG (Simonyan & Zisserman, 2015) network. Specifically, we use layers conv3_1 ($256 \times 32 \times 32$), conv4_1 ($512 \times 16 \times 16$) and conv5_1 ($512 \times 8 \times 8$),

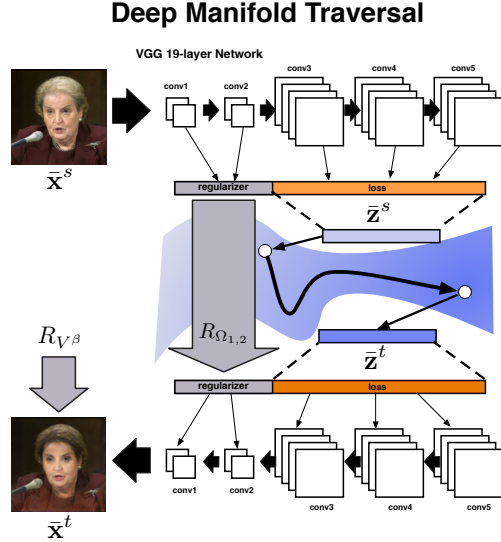


Figure 2: Deep manifold traversal via $\bar{\mathbf{x}}^s \rightarrow \bar{\mathbf{z}}^s \rightarrow \bar{\mathbf{z}}^t \rightarrow \bar{\mathbf{x}}^t$. **Top:** The input image $\bar{\mathbf{x}}^s$ is transformed by VGG, a ConvNet to deep neural features (orange) which are PCA projected to manifold space (blue). **Middle:** The manifold is traversed (black arrow) from source-to-target to latent position $\bar{\mathbf{z}}^t$. **Bottom:** $\bar{\mathbf{z}}^t$ is inverted to recover $\bar{\mathbf{x}}^t$, subject to two regularizers, $R_{\Omega_{1,2}}$ and R_{V^β} .

which have the indicated dimensionalities when the color input is 125×125 . These layers are the first convolutions in the 3rd, 4th and 5th pooling regions. After ReLU, flattening and concatenation, a feature vector has 425984 dimensions.

Dimensionality reduction. The extracted feature vector is sparse but of very high dimensionality. To reduce the degrees of freedom when changing an image and capture the sub-manifold of images of interest, we reduce the dimensionality using PCA. Since we want to demonstrate our method on images of faces we use 13143 images from the Labeled Faces in the Wild dataset (Huang et al., 2007; Huang & Learned-Miller, 2014) as training data for PCA. The resulting mapping of an image \mathbf{x} to this lower dimensional representation becomes

$$\mathbf{z} := \phi(\mathbf{x}) = \mathbf{U}^\top \Omega_{3,4,5}(\mathbf{x}) \quad (4)$$

where $\Omega(\cdot)$ extracts convolutional features and \mathbf{U} is the PCA projection matrix. We map all of our source images $\mathbf{x}_i^s \rightarrow \mathbf{z}_i^s$, target images $\mathbf{x}_i^t \rightarrow \mathbf{z}_i^t$, and input image $\bar{\mathbf{x}}^s \rightarrow \bar{\mathbf{z}}^s$ in this way.

Image transformation. Intuitively, our approach to image transformation will be to change the deep visual features $\bar{\mathbf{z}}^s$ to look more like the deep visual features characteristic of those training images with target label y^t . This transformation is guided by the MMD witness function from section 3. We make use of the empirical witness function $f^*(\mathbf{z})$ to measure the degree to which some \mathbf{z} resembles objects with source label y^s or those with target label y^t :

$$f^*(\mathbf{z}) = \sum_{i=1}^s k(\mathbf{z}_i^s, \mathbf{z}) - \sum_{i=1}^t k(\mathbf{z}_i^t, \mathbf{z}). \quad (5)$$

Note that, while kernel methods often generalize poorly on images in pixel space because of isolated smoothness assumptions, we expect that these assumptions hold after deep visual feature extraction (Bengio et al., 2007).

The witness function $f^*(\mathbf{z})$ has a negative value if \mathbf{z} encodes deep visual features more characteristic of label y^t than of label y^s . To transform $\bar{\mathbf{x}}^s$ to have target label y^t , we therefore wish to minimize $f^*(\bar{\mathbf{z}}^s + \delta)$ in δ . However, when performed unbounded, this optimization moves too far along the manifold to a mode of the target domain, preserving little of the information contained in $\bar{\mathbf{z}}^s$. We therefore follow the techniques used in Szegedy et al. (2013b) and enforce a *budget* of change, and instead obtain $\bar{\mathbf{z}}^t$ by minimizing:

$$\bar{\mathbf{z}}^t = \bar{\mathbf{z}}^s + \delta \quad \text{where: } \delta = \arg \min_{\delta} f^*(\bar{\mathbf{z}}^s + \delta) + \lambda \|\delta\|_2^2. \quad (6)$$

It worth emphasizing that minimizing the witness function encodes two “forces”: $\bar{\mathbf{z}}^t$ is pushed *away* from visual features characteristic of the source label y^s and simultaneously pulled *towards* visual features characteristic of the target label y^t . Viewed as a Lagrange multiplier, the hyperparameter λ encodes a budget of how much we allow the optimization to modify $\bar{\mathbf{z}}^s$. While in image transformation the choice of this parameter is largely subjective, we expect many applications of label transformations to have real budgets that must be satisfied.¹

Reconstruction. The optimization results in the transformed representation in the low dimensional manifold space, $\bar{\mathbf{z}}^t$. In order to obtain our corresponding target image $\bar{\mathbf{x}}^t = \phi^{-1}(\bar{\mathbf{z}}^t)$ in pixel space we need to invert the mapping $\phi(\bar{\mathbf{x}}^t) = \mathbf{U}\Omega_{3,4,5}(\bar{\mathbf{x}}^t)$. Since PCA is an invertible projection, we can apply \mathbf{U} to recover deep visual features $\mathbf{U}\bar{\mathbf{z}}^t$. The deep ConvNet mapping is not invertible, so we cannot obtain the image in pixel space $\bar{\mathbf{x}}^t$ from $\mathbf{U}\bar{\mathbf{z}}^t$ directly. The mapping is however differentiable and we can adopt the approaches of Mahendran & Vedaldi (2015) and Gatys et al. (2015) to find $\bar{\mathbf{x}}^t$ with gradient descent by minimizing the loss function

$$L_{\Omega_{3,4,5}}(\bar{\mathbf{x}}^t) = \frac{1}{2} \|\Omega_{3,4,5}(\bar{\mathbf{x}}^t) - \mathbf{U}\bar{\mathbf{z}}^t\|^2. \quad (7)$$

¹In practice, the parameter λ could be set automatically with constrained Bayesian optimization (Gardner et al., 2014; Gelbart et al., 2014).

Regularization. The VGG network contains five pooling regions and all layers of the 1st and 2nd pooling regions are not represented directly in $\Omega_{3,4,5}$. Therefore, the minimization in (7) is underconstrained, which results in images with visual artifacts (e.g., color blotches and noise) due to unintended degrees of freedom (see Figure 4). We therefore introduce two additional regularizers to our objective. The first one keeps the 1st and 2nd pooling region features of $\bar{\mathbf{x}}^t$ close to those of the input image, $\bar{\mathbf{x}}^s$. Let $\Omega_{1,2}(\bar{\mathbf{x}}^s)$ be the conv1_1 and conv2_1 features of $\bar{\mathbf{x}}^s$. Then our first regularizer is

$$R_{\Omega_{1,2}}(\bar{\mathbf{x}}^t) = \frac{1}{2} \|\Omega_{1,2}(\bar{\mathbf{x}}^t) - \Omega_{1,2}(\bar{\mathbf{x}}^s)\|^2.$$

The output image also contains “spike” artifacts. Mahendran & Vedaldi (2015) observed this and found that a total variation regularizer,

$$R_{V^\beta}(\bar{\mathbf{x}}^t) = \sum_{i,j} \left((x_{i,j+1} - x_{i,j})^2 + (x_{i+1,j} - x_{i,j})^2 \right)^{\frac{\beta}{2}}$$

reduces spikes. Here, $x_{i,j}$ refers to the pixel with i, j coordinate in image \mathbf{x} . The addition of these two regularizers greatly improves image quality. The final optimization problem becomes

$$\bar{\mathbf{x}}^t = \arg \min_{\bar{\mathbf{x}}^t} L_{\Omega_{3,4,5}}(\bar{\mathbf{x}}^t) + \lambda_{\Omega_{1,2}} R_{\Omega_{1,2}}(\bar{\mathbf{x}}^t) + \lambda_{V^\beta} R_{V^\beta}(\bar{\mathbf{x}}^t). \quad (8)$$

We minimize (8) with bounded L-BFGS initialized with $\bar{\mathbf{x}}^s$. We set $\lambda_{\Omega_{1,2}} = 0.02$, $\lambda_{V^\beta} = 0.001$ and $\beta = 2$ in our experiments. Reconstructing a 125×125 color image takes 114 seconds on an NVIDIA Tesla K40 GPU. After reconstruction we have completed the manifold traversal $\bar{\mathbf{x}}^s \rightarrow \bar{\mathbf{z}}^s \rightarrow \bar{\mathbf{z}}^t \rightarrow \bar{\mathbf{x}}^t$.

5 EXPERIMENTAL RESULTS

We evaluate our method on several manifold traversal tasks using the Labeled Faces in the Wild (LFW) dataset. This dataset contains 13143 images of faces with annotations for 73 different classes (e.g., “sunglasses”, “soft lighting”, “round face”, “curly hair”, “mustache”, etc.). Annotations provide ground truth which is needed to construct source and target image sets which perform a known task. However, the LFW annotations are the output of a machine learning classifier (Kumar et al., 2009) which have label noise. Therefore, we take the 2000 most confidently labeled images to construct an image set. For example, in our aging task below, we take the bottom (i.e., most negative) and top (i.e., most positive) 2000 images in the “senior” class as our source and target image sets. For the reverse task of making the person younger, we simply reverse these sets.

Manifold traversal demonstration. In figure 1, we display several examples of manifold traversal using our algorithm superimposed on a cartoon illustration of two manifolds². This figure presents four tasks in total. For Harrison Ford, we traverse the manifold to change the true label to “older”, “younger”, and “frowning”. For Madeleine Albright, we change to “younger”.

Overall, the visual quality of the transformed photographs is high (these photographs may be zoomed in on for further detail). In both of the “younger” tasks, the hair color in the original image was changed to be darker, and the algorithm smoothed out wrinkles and bags under the eyes. In the “frowning” transformation, Harrison Ford is now frowning. The “aging” transformation made Harrison Ford’s hair lighter and added wrinkles to his face.

Critically, neither the background nor the clothes were altered significantly in any image. This deviates from what one would expect by, for example, simply interpolating between the original image and an average of known images of the target label. This is strong evidence that our algorithm only makes changes that are *necessary for the task at hand*.



Without Regularization With Regularization
Figure 3: The effect of regularization on the reconstructive optimization.

²Many of the figures in this paper are best viewed in color on a computer screen. In particular, the faces in figure 1 may be zoomed in on for additional detail



Figure 5: **Top row:** Input grayscale images. **Bottom row:** Targeted colorization of the face with correct skin tone by seeking a mode of the multimodal target domain. We do not use masks to target the face — the targeting is learned unsupervised. Zoom in for details.

Image transformation between specific people. Can we learn a meaningful transformation between two completely different people? As in the previous section we can think of each person having their own manifold of images which describe subtle variations in age, emotions, and hairstyle, among others. Additionally, there exists a larger *face manifold* that describes all face images, in which each specific person’s manifold is embedded. The question posed by this experiment is to see if we can traverse from one person’s manifold to another while remaining close to the face manifold.

Figure 4 shows the result of our method when used to transform multiple images from their manifold to that of George W. Bush. We see that our technique makes small but important changes that make the image look more like George W. Bush while maintaining background and clothing.

Semantic understanding. Correct colorization of a grayscale image requires understanding semantic cues. Can our method colorize the face? The target domain is images annotated as “color photo”. Although the attribute label is “color photo”, the target domain is actually color faces since PCA projects out features unrelated to faces. Due to the scarcity of grayscale images, we only use 200 images in the source domain. We present results for four celebrities which do not have any color images in LFW in figure 5.

Our method produced the correct skin tone for all four celebrities and the colorization is mostly constrained to the face. Clothing, background, ears, and hair are less colorized. No changes are made to facial structure, age, facial expression, and hairstyle. Our method learns to target the face — supervised masks of facial regions are not used during training. This experiment demonstrates that the changes made *preserve information irrelevant to the change*. Furthermore, the skin tone domain is clearly multimodal and our method correctly seeks nearby modes rather than merely moving toward a global mean image in the target domain.

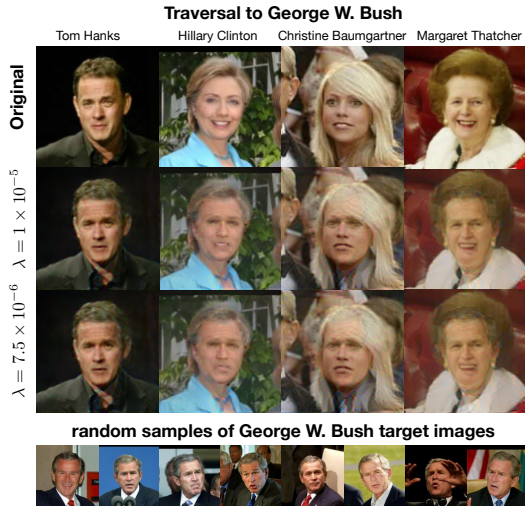


Figure 4: Manifold traversal towards George W. Bush. Our method is able to make meaningful changes from an arbitrary person’s manifold to that of George W. Bush.

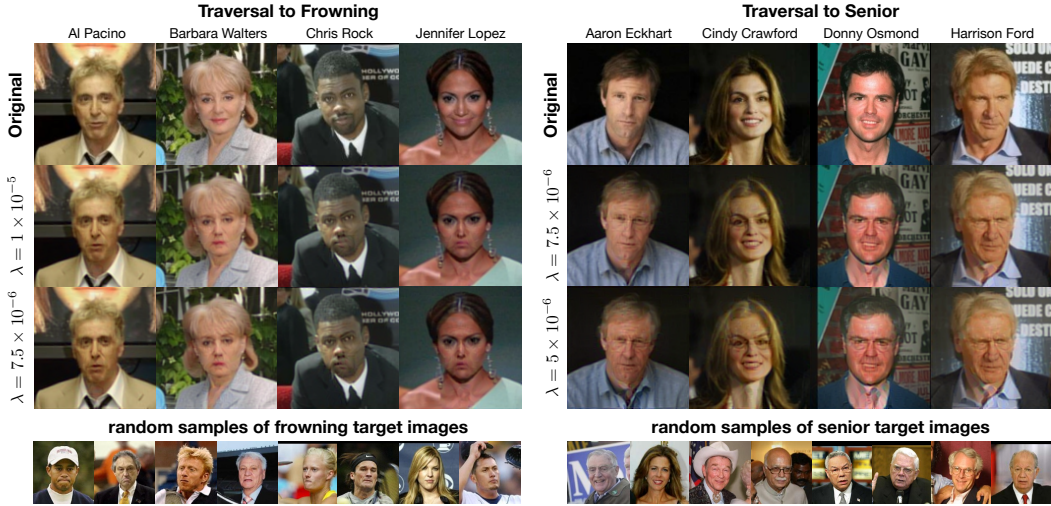


Figure 6: **Top row:** Original images. **Middle and bottom rows:** Controlled manifold traversals by varying λ . A smaller λ produces a more prominent effect (e.g., downturned frowns, gray hair, bags under the eyes). Zoom in for details.

Controlled manifold traversal. The λ parameter allows us to control the degree of transformation. What is the effect of λ ? In figure 6 we look at two tasks: frowning and aging for a diverse set of hair styles, lighting, gender, clothing and background. For each task, four different celebrity images were made to frown (look older) by traversing their personalized manifold to the portion closer to the “frowning” (“senior”) annotated faces. The top row is the original image which corresponds to $\lambda = \infty$. Bottom rows are manifold traversals with the indicated λ values.

At different values of λ the smiles of Al Pacino and Barbara Walters become neutral expressions or frowns. The effect of λ on Jennifer Lopez is particularly dramatic with her cheery smile becoming an extreme frown pulling her entire lower face downward. λ also has a dramatic aging effect on Aaron Eckhart and Harrison Ford: their hair becomes completely gray, bags appear beneath their eyes and excessive wrinkles give them a weathered look. The aging effect is less strong on Cindy Crawford with her becoming lighter in color and wrinkles deepening.

Our method is able to make meaningful changes tailored to each image simply by varying λ . In all cases the background is unchanged. Clothes are unchanged by frowning but begins to change for low λ on the aging task.

t-SNE visualization of image transformations. We want to visualize the manifold traversal trajectory. Because we cannot visualize high-dimensional spaces directly we use a prominent visualization technique called t-Stochastic Neighbor Embedding (t-SNE) Van der Maaten & Hinton (2008). t-SNE visualizes high-dimensional datasets in two or three dimensions by learning an embedding such that if points are close in the low-dimensional visualization then they are likely to be close in the original space.

Figure 7 shows a t-SNE visualization of a subset of the LFW dataset (with 50 “senior” faces and 50 non-“senior” faces, randomly sampled from each category). We track three points along a manifold traversal. The closest neighbors of the input image are largely non-“senior” images. As we traverse the manifold, the neighbors of the learned image become increasingly “senior”. This indicates that we are truly traversing a meaningful latent manifold during our optimization procedure.

6 CONCLUSION

In this paper, we have introduced the novel machine learning task of *actionable change*. This is a task that traditional machine learning techniques—from linear models to powerful deep neural networks—almost universally fail at, yet has the potential to dramatically improve the usefulness of

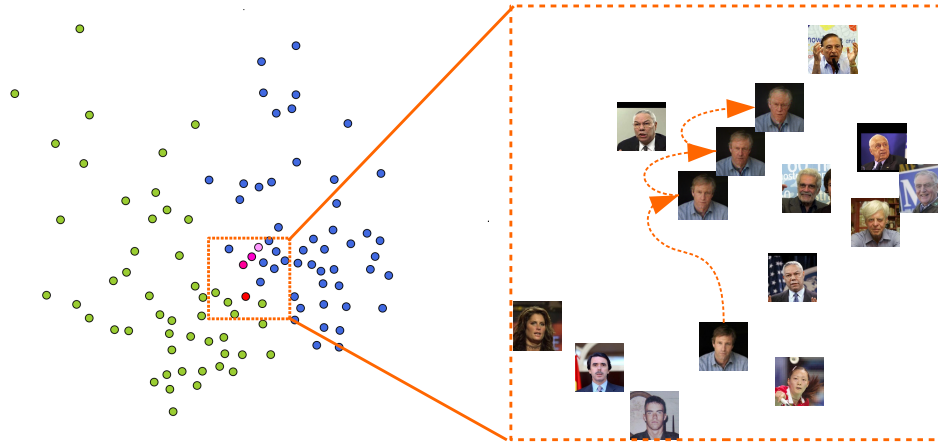


Figure 7: **Left:** colored points are locations in the latent low-dimensional PCA space, embedded in 2-d by t-SNE. Blue points are labeled “senior” and green points are non-“senior”. The red points near the center track an input image and three points along a manifold traversal towards the “senior” class. **Right:** a zoomed in view of the boxed region. Arrows indicate the manifold traversal. Zoom in for details.

machine learning in many fields. We have proposed a framework based on deep manifold traversal for making *actionable, meaningful changes* to the *true label* of a source instance, and validated our framework on several image transformation tasks. Although many of these image transformation tasks have specific tools developed in computer vision, we emphasize that our framework is completely general, requiring only a set of labeled examples of the current and target true labels. We believe there are many directions for future work including extending this work to different application settings, developing rigorous theory behind actionable change, and better handling scenarios where movement *between* manifolds is necessary. One could also imagine to use our approach to sample new images within the same class as the source images, which could be used as additional training samples for discriminative classifiers.

REFERENCES

- Bengio, Yoshua, LeCun, Yann, et al. Scaling learning algorithms towards ai. *Large-scale kernel machines*, 34(5), 2007.
- Bitouk, Dmitri, Kumar, Neeraj, Dhillon, Samreen, Belhumeur, Peter, and Nayar, Shree K. Face swapping: automatically replacing faces in photographs. *ACM Transactions on Graphics (TOG)*, 27(3):39, 2008.
- Chia, Alex Yong-Sang, Zhuo, Shaojie, Gupta, Raj Kumar, Tai, Yu-Wing, Cho, Siu-Yeung, Tan, Ping, and Lin, Stephen. Semantic colorization with internet images. In *ACM Transactions on Graphics (TOG)*, volume 30, pp. 156. ACM, 2011.
- Cruz-Roa, Angel Alfonso, Ovalle, John Edison Arevalo, Madabhushi, Anant, and Osorio, Fabio Augusto González. A deep learning architecture for image representation, visual interpretability and automated basal-cell carcinoma cancer detection. In *Medical Image Computing and Computer-Assisted Intervention–MICCAI 2013*, pp. 403–410. Springer, 2013.
- Cui, Zhicheng, Chen, Wenlin, He, Yujie, and Chen, Yixin. Optimal action extraction for random forests and boosted trees. In *Proceedings of the 21th ACM SIGKDD International Conference on Knowledge Discovery and Data Mining*, pp. 179–188. ACM, 2015.
- Donahue, Jeff, Jia, Yangqing, Vinyals, Oriol, Hoffman, Judy, Zhang, Ning, Tzeng, Eric, and Darrell, Trevor. Decaf: A deep convolutional activation feature for generic visual recognition. *arXiv preprint arXiv:1310.1531*, 2013.

- Fortet, Robert and Mourier, E. Convergence de la répartition empirique vers la répartition théorique. *Annales scientifiques de l'École Normale Supérieure*, 70(3):267–285, 1953.
- Gardner, Jacob, Kusner, Matt, Xu, Zhixiang, Weinberger, Kilian, and Cunningham, John. Bayesian optimization with inequality constraints. In *Proceedings of the 31st International Conference on Machine Learning (ICML-14)*, pp. 937–945, 2014.
- Gatys, Leon A, Ecker, Alexander S, and Bethge, Matthias. A neural algorithm of artistic style. *arXiv preprint arXiv:1508.06576*, 2015.
- Gelbart, Michael A, Snoek, Jasper, and Adams, Ryan P. Bayesian optimization with unknown constraints. *arXiv preprint arXiv:1403.5607*, 2014.
- Goodfellow, Ian J, Shlens, Jonathon, and Szegedy, Christian. Explaining and harnessing adversarial examples. *arXiv preprint arXiv:1412.6572*, 2014.
- Gretton, Arthur, Borgwardt, Karsten M, Rasch, Malte, Schölkopf, Bernhard, and Smola, Alex J. A kernel method for the two-sample-problem. In *Advances in neural information processing systems*, pp. 513–520, 2006.
- Gretton, Arthur, Borgwardt, Karsten M, Rasch, Malte J, Schölkopf, Bernhard, and Smola, Alexander. A kernel two-sample test. *The Journal of Machine Learning Research*, 13(1):723–773, 2012.
- Hadsell, Raia, Sermanet, Pierre, Ben, Jan, Erkan, Ayse, Scoffier, Marco, Kavukcuoglu, Koray, Muller, Urs, and LeCun, Yann. Learning long-range vision for autonomous off-road driving. *Journal of Field Robotics*, 26(2):120–144, 2009.
- He, Kaiming, Zhang, Xiangyu, Ren, Shaoqing, and Sun, Jian. Delving deep into rectifiers: Surpassing human-level performance on imagenet classification. *arXiv preprint arXiv:1502.01852*, 2015.
- Huang, Gary B. and Learned-Miller, Erik. Labeled faces in the wild: Updates and new reporting procedures. Technical Report UM-CS-2014-003, University of Massachusetts, Amherst, May 2014.
- Huang, Gary B., Ramesh, Manu, Berg, Tamara, and Learned-Miller, Erik. Labeled faces in the wild: A database for studying face recognition in unconstrained environments. Technical Report 07-49, University of Massachusetts, Amherst, October 2007.
- Kemelmacher-Shlizerman, Ira. Internet based morphable model. In *Computer Vision (ICCV), 2013 IEEE International Conference on*, pp. 3256–3263. IEEE, 2013.
- Kemelmacher-Shlizerman, Ira, Suwajanakorn, Supasorn, and Seitz, Steven M. Illumination-aware age progression. In *Computer Vision and Pattern Recognition (CVPR), 2014 IEEE Conference on*, pp. 3334–3341. IEEE, 2014.
- Krizhevsky, Alex, Sutskever, Ilya, and Hinton, Geoffrey E. Imagenet classification with deep convolutional neural networks. In *Advances in neural information processing systems*, pp. 1097–1105, 2012.
- Kumar, N., Berg, A. C., Belhumeur, P. N., and Nayar, S. K. Attribute and simile classifiers for face verification. In *IEEE International Conference on Computer Vision (ICCV)*, Oct 2009.
- Li, Yujia, Swersky, Kevin, and Zemel, Richard. Generative moment matching networks. *arXiv preprint arXiv:1502.02761*, 2015.
- Mahendran, Aravindh and Vedaldi, Andrea. Understanding deep image representations by inverting them. In *Proceedings of the IEEE Conf. on Computer Vision and Pattern Recognition (CVPR)*, 2015.
- Nguyen, Anh, Yosinski, Jason, and Clune, Jeff. Deep neural networks are easily fooled: High confidence predictions for unrecognizable images. *arXiv preprint arXiv:1412.1897*, 2014.

- Razavian, Ali S, Azizpour, Hossein, Sullivan, Josephine, and Carlsson, Stefan. Cnn features off-the-shelf: an astounding baseline for recognition. In *Computer Vision and Pattern Recognition Workshops (CVPRW), 2014 IEEE Conference on*, pp. 512–519. IEEE, 2014.
- Russakovsky, Olga, Deng, Jia, Su, Hao, Krause, Jonathan, Satheesh, Sanjeev, Ma, Sean, Huang, Zhiheng, Karpathy, Andrej, Khosla, Aditya, Bernstein, Michael, Berg, Alexander C., and Fei-Fei, Li. ImageNet Large Scale Visual Recognition Challenge. *International Journal of Computer Vision (IJCV)*, 115(3):211–252, 2015. doi: 10.1007/s11263-015-0816-y.
- Sermanet, Pierre, Eigen, David, Zhang, Xiang, Mathieu, Michaël, Fergus, Rob, and LeCun, Yann. Overfeat: Integrated recognition, localization and detection using convolutional networks. *arXiv preprint arXiv:1312.6229*, 2013.
- Simonyan, Karen and Zisserman, Andrew. Very deep convolutional networks for large-scale image recognition. In *International Conference on Learning Representations*, 2015.
- Szegedy, Christian, Toshev, Alexander, and Erhan, Dumitru. Deep neural networks for object detection. In *Advances in Neural Information Processing Systems*, pp. 2553–2561, 2013a.
- Szegedy, Christian, Zaremba, Wojciech, Sutskever, Ilya, Bruna, Joan, Erhan, Dumitru, Goodfellow, Ian, and Fergus, Rob. Intriguing properties of neural networks. *arXiv preprint arXiv:1312.6199*, 2013b.
- Van der Maaten, Laurens and Hinton, Geoffrey. Visualizing high-dimensional data using t-sne. *Journal of Machine Learning Research*, 9:2579–2605, 2008.
- Weinberger, Kilian Q and Saul, Lawrence K. Unsupervised learning of image manifolds by semidefinite programming. *International Journal of Computer Vision*, 70(1):77–90, 2006.
- Yu, Shipeng, Van Esbroeck, Alexander, Farooq, Fahad, Fung, Glenn, Anand, Vishal, and Krishnapuram, Balaji. Predicting readmission risk with institution specific prediction models. In *Healthcare Informatics (ICHI), 2013 IEEE International Conference on*, pp. 415–420. IEEE, 2013.